2

A Study of Adhesion of Silicon Dioxide on Polymeric Substrates for Optoelectronic Applications

E. Amendola[1,2], A. Cammarano[2] and D. Acierno[3]
[1]*Institute of Composite and Biomedical Materials, National Research Council, Piazzale E. Fermi 1, 80055 Portici (NA),*
[2]*Technological District of Polymer and Composite Materials Engineering and Structures, IMAST S.c.a.r.l, Piazzale E.Fermi 1, 80055 Portici (NA),*
[3]*Department of Materials and Production Engineering, University of Naples "Federico II", Piazzale Tecchio 80, 80125 Naples*
[1,2,3]*Italy*

1. Introduction

The use of plastic film substrates for organic electronic devices promises to enable new applications.
Plastic substrates have several advantages, such as ruggedness, robustness, ultra lightness, conformability and impact resistance over glass substrates, which are primarily used in flat panel displays (FPDs) today (Imparato et al., 2005). However, high transparency, proper surface roughness, low gas permeability and highly transparent electrode conductivity of the plastic substrate are required for commercial applications (Choi et al., 2008) (Mannifacier et al., 1979) (Adhikari & Majumdar, 2004).
Polyesters, both amorphous and semicrystalline, are a promising class of commercial polymers for optoelectronic applications.
Despite the best premises, the adoption of polymers for electronic applications has been slowed by their limited compatibility with semiconductor fabrication processes, at least during the first stage of the transition towards all-polymeric functional devices. In particular, the relatively high linear expansion coefficient, α, and low glass transition temperature, Tg, of most polymers limit their use to temperatures above 250°C. Therefore, the high-temperature process leads to considerable mechanical stress and difficulties in maintaining accurate alignment of features on the plastic substrate.
The availability of suitable polymeric functional materials, with reliable and durable performances, will eventually results in development of fully polymeric devices, with milder processing requirements in term of high temperature exposure.
At the present stage, inorganic materials are used as buffer, conductive and protective layers for functional organics and high performance polymer substrates.
Several high-Tg polymers (Tg >220°C) with optical transparency, good chemical resistance and barrier properties have recently been developed for applications in organic display technology, and these latest developments have motivated the present research.

Ferrania Imaging Technologies, has developed amorphous polyester material, AryLite™, with high glass transition temperature (Tg ≈ 320°C) and good optical transparency (Angiolini & Avidano, 2001).
Substrates for flexible organic electronic devices are multilayer composite structures comprising a polymer-based substrate on which are deposited a number of functional coatings, with specific roles:

- chemical protection from the hostile environment during processing;
- mechanical protection, such as improvement of the scratch resistance;
- a diffusion (or permeation) barrier. A polymer based permeation barrier may be sufficient for protection during, for instance, processing during display manufacturing;
- electrical connections.

Taking into account that for a number of these functions transparent coatings are required, silicon dioxide (SiO_2) layer has been deposited on AryLite™ substrate at temperatures below 50°C in an Electron Cyclotron Resonance (ECR) plasma reactor from H_2, SiH_4, and N_2O gas mixture. Silicon dioxide possesses excellent physical and chemical properties, such as transparency from ultraviolet to infrared, good thermal stability, chemical inertness, wear and corrosion resistance and low gas permeation.
In a multilayer structure, the adhesion between organic/inorganic layer plays an important role in determining the reliability of the optoelectronic devices.
As a matter of fact, the effort is focused on the improvement of adhesion between organic-inorganic materials, and the use of nanocomposite (hybrid) substrates (Amendola et al., 2009).
Adhesion properties can be varied by modifying the surface, by means of several chemical and/or physical processes (Goddard & Hotchkiss, 2007).
The most common techniques include plasma-ion beam treatment, electric discharge, surface grafting, chemical reaction, metal vapour deposition, flame treatment, and chemical oxidation. In this way it's possible to change hydrophobic polymer surface into a hydrophilic one without affecting the bulk properties.
Adhesion can be improved also by using an adhesion promoter such as a silane on the polymer surface. In this work the surface of polyester films was modified via chemical solution. Afterward, samples have been treated with (3-Aminopropyl)triethoxysilane (APTEOS) that function as an adhesion promoter between organic substrate and SiO_2 layer. In particular, SiOH silane functional groups are suitable for coupling with SiO_2 layer.
Contact angle and roughness measurements, surface free energy calculation and attenuated total reflectance Fourier transform infrared spectroscopy (ATR-FTIR) were used to monitor the effects of silane treatments on the physical and chemical characteristics of pristine and modified polyester surfaces. Infrared spectroscopic analysis has been performed in order to study the reaction between amino group present on the organosilane backbone and carbonilic group of polyester substrate.
Conventional characterization techniques are not appropriate for the measurement of mechanical and adhesion properties of thin functional layers on substrate. Nano-indentation and nano-scratch testing are alternative approaching methods. Both techniques have become important tools for probing the mechanical properties of small volumes of material at the nano-scale.
Indentation measurements has been used to evaluate the hardness and Young's modulus of films. The film adhesion was determined by the nano-scratch test.

2. Materials

AryLite™ (supplied by Ferrania Imaging Technologies S.p.A.) characterised by very high glass transition temperature, has been selected due to its outstanding thermo-mechanical and optical properties. Polymer films of 10 cm x 10 cm and of 100 μm in thickness have been used.
Silicon dioxide (SiO_2) layers were deposited at temperatures below 50 °C in an electron cyclotron resonance (ECR) plasma reactor from N_2O, SiH_4, and H_2 gas mixture.
Coupling agent with amino functional group (3-Aminopropyl)triethoxysilane (APTEOS) has been supplied by Aldrich and used without further purification.

3. Method

3.1 Thermo-Mechanical properties of substrates

Thermal properties of substrates under investigation have been evaluated in order to determine glass transition temperature Tg and degradation temperature by differential scanning calorimetry (DSC) and thermogravimetric analysis (TGA) respectively.
The glass transition (Tg) was investigated by DSC-Q1000 (TA Instruments). The DSC thermal analysis technique measures heat flows and phase changes on a sample under thermal cycles. Since the Tg of AryLite™ is overlaid by an enthalpic relaxation phenomenon, deeper investigations were performed with Modulated DSC (MDSC).
Enthalpic relaxation is an endothermic process that can vary in magnitude depending on the thermal history of the material. Traditional DSC measures the sum of all thermal events in the sample. When multiple transitions occur in the same temperature range, results are often confusing and misinterpreted. MDSC eliminates this problem by separating the total heat flow signal into two separated contribution, namely "Reversing" and "Non Reversing". The reversing signal provides information on heat capacity and melting, while the non reversing signal shows the kinetic process of enthalpic recovery and cold crystallization.
In MDSC analysis, the samples were heated from 150 °C to 400 °C, at heating rate of 2.5 °C/min, with a modulated temperature amplitude of 0.5 °C and a period of 60 sec under a nitrogen flow.
The degradation temperature and thermal stability were investigated by thermogravimetric analysis TGA-Q5000 (TA Instruments). The weight loss due to the formation of volatile products caused by the degradation at high temperature was monitored as a function of temperature. The heating occurred both under a nitrogen and oxygen flow, from room temperature up to 900°C with a heating rate of 10 °C/min.
Elastic modulus and ultimate properties were investigated according to UNI EN ISO 527-3 on rectangular specimens with 150 mm length, 25 mm width and 0.1 mm thick using a mechanical dynamometer SANS 4023 with a 30 kN loading cell and a traverse speed of 20mm/min.

3.2 Surface treatments

3.2.1 Surface modification by coupling reactions

Polymer films were preliminary immersed in an alcohol/water (1/1, v/v) solution for 2 h in order to clean the surface and then rinsed with a large amount of distilled water. They were dried under reduced pressure for 12 h at 25 °C.
AryLite™ samples have been functionalized with (3-Aminopropyl)triethoxysilane. Untreated AryLite™ samples have been used as substrate for the sake of comparison.

Prior to AryLite™ surface treatments, the SiOR groups of the silane were transformed to active SiOH groups for the subsequent condensation reactions. The transformation is realized by hydrolyzing the silane in a aqueous solution. 7.5 wt % silane solution were prepared by adding the silane to a mixture of 70:30 ethanol and distilled water. The pH of the solution was adjusted to 5.5 by inclusion of a few droplet of acetic acid. The solution was stirred for 10 minutes and the system was kept 1 h at room temperature for hydrolysis reaction and silanol formation. Subsequently the films were dipped into the solution for 30 minutes at room temperature.
These silane-treated specimens were rinsed with distilled water to eliminate the unreacted silane and dried under reduced pressure at 25°C overnight.
Reaction path is reported in figure 1.
The reaction proceeds through a nucleophilic attack of NH_2 nitrogen atom to the carbon atom of carbonilic group generating an amide group.

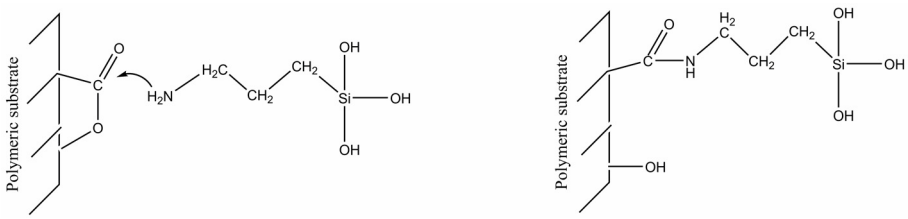

Fig. 1. Scheme of nucleophilic addition of NH_2 group to the polyester carbonilic group

3.2.2 Electron Cyclotron Resonance (ECR) deposition

The deposition process was performed by ENEA Portici research centre (Naples) using Multichamber System MC5000, a Ultra High Vacuum Multichamber for Plasma Enhanced Chemical Vapour Deposition.
Thousand nm thick SiO_2 layer was deposited by Electron Cyclotron Resonance (ECR) on a single face of AryLite™ substrate. During deposition process gas flows are kept constant at 2 sccm (standard cubic centimeters per minute) for SiH_4, 70 sccm for H_2 and 40 sccm for N_2O.
Deposition was performed for 13 minutes setting magnetron power to 400 W. Samples were heated at 50°C under hydrogen flow for 5 minutes before SiO_2 deposition. Films were purged under nitrogen flow for 5 minutes at the end of the treatment.

3.3 Spectroscopic analysis FTIR-ATR

Infrared spectroscopic analysis has been performed by Nicolet Nexus 670 FTIR equipped with attenuated total reflection (ATR) smart ARK HATR accessory.
In ATR, the sample is placed in optical contact on a zinc selenide (ZnSe) crystal. The IR beam penetrate a short distance into the sample. This penetration is termed the evanescent wave. The sample interacts with the evanescent wave, resulting in the absorption of radiation by the sample, which closely resembles the transmission spectrum for the same sample. However, the ATR spectrum will depend upon several parameters, including the angle of incidence (θ) for the incoming radiation, the wavelength of the radiation (λ), and the refractive indices of the sample (n_2) and the ATR crystal (n_1). The penetration depth (d_p) of the evanescent wave, is defined by equation 1.

$$d_p = \frac{\lambda}{2\pi(n_1^2 sen^2\theta - n_2^2)^{1/2}} \quad (1)$$

In the 400 – 4800cm^{-1} wavenumber investigated range, d_p varies from 5 μm to 15 μm for measured substrates (Zuwei et al., 2007).
A spectroscopic investigation has been performed, also, by using a transmitted infrared analysis to verify the kind of chemical reaction that occurs between polymer substrate and organosilane.
The sample for FTIR analysis has been prepared by adding the amminosilane in a polyarilate solution in dichloromethane solvent. In this way After treatment, films have been obtained by solvent casting technique. They have been heated at 100 °C for 1 h in order to remove the whole solvent. Treated films finely divided, were ground and dispersed in a matrix of KBr (300 mg), followed by compression at 700 MPa to consolidate the formation of the pellet for FTIR measurements.
All spectra were recorded in the range of 4000–800 cm^{-1}.

3.4 Contact angle measurements

Contact angle measurements have been used to verify chemical surface modification. The surface wettability was evaluated by contact angle measurements using the sessile drop method (Mack, 1936) considering the shape of the small liquid drop to be a truncated sphere. Prior to contact angle measurement, samples were washed in ethanol and deionised water.
Contact angles were obtained using a Dataphysics OCA-20 contact angle analyzer with 1 μL of liquid. A digital drop image has been processed by an image analysis system, which calculated both the left and right contact angles from the shape of the drop with an accuracy of ±0.1°. Drop contact angle were used to assess efficiency of surface modification suffered by the polymer films. Each solid sample was measured ten times with liquid at room temperature. The contact angle data were obtained at room temperature using two different liquids: water and ethylene glycol (Ozcan & Hasirci, 2008). The contact angle is a method for evaluation of the solid surface free energy (SFE) (van Oss et al., 1988).

3.5 Evaluation of surface free energy (SFE)

The values of SFE were obtained at room temperature using two liquids (Cantin et al., 2006) with known surface tension (table 1). Two liquids with different polarity (P) have been selected: water and ethylene glycol. The liquids, supplied by Aldrich, were used without further purification.
Surface free energy of the polymer substrates was calculated using the methods proposed by Owens and Wendt (1969) which divide the total surface free energy (γ) in 2 parts: dispersive (γ_s^d) and polar (γ_s^P). The dispersive component accounts for all the London forces such as dispersion (London–van der Waals), orientation (Keesom–van der Waals), induction (Debye–van der Waals) and Lifshitz–van der Waals (LW) forces. The polar component is affected by hydrogen bonding components.
The theory of contact angle of pure liquids on a solid was developed nearly 200 years ago in terms of the Young equation (1805):

$$\gamma_L \cos\theta = \gamma_S + \gamma_{SL} \quad (2)$$

	Surface tension [mJ/m²] and Polarity			
	γ	γ_L^d	γ_L^p	P
Distilled Water	72.8	21.8	51	0.70
Ethylene Glycol	48	29	19	0.40

Table 1. Surface tension data of test liquids (Ozcan & Hasirci, 2008)

where γ_L is the experimentally determined surface tension of the liquid, θ is the contact angle, γ_S is the surface free energy of the solid and γ_{SL} is the solid–liquid interfacial energy. In order to obtain the solid surface free energy γ_S an estimate of γ_{SL} has to be done. Fowkes (1962) pioneered a surface free energy component approach. He divided the total surface free energy in 2 parts: dispersive part and non-dispersive (or polar) part. Owens and Wendt (1969) extended the Fowkes equation and included the hydrogen bonding term. They used geometric mean to combine the dispersion force and hydrogen bonding components:

$$\gamma_{SL} = \gamma_S + \gamma_L - 2\sqrt{\gamma_S^d \gamma_L^d} - 2\sqrt{\gamma_S^p \gamma_L^p} \tag{3}$$

Dispersion force and polar components are indicated respectively by superscript *d* and *p*. From the Young equation it follows that:

$$\gamma_L(1+\cos\theta) = 2\sqrt{\gamma_S^d \gamma_L^d} + 2\sqrt{\gamma_S^p \gamma_L^p} \tag{4}$$

In order to obtain γ_S^d and γ_S^p of a solid, contact angle data for a minimum of two known liquids are required. If two liquids are used, then, one must be polar and the other is non-polar.

3.6 Topography measurements

Topography measurements were performed in this studies in order to investigate the roughness of polyester films before and after surface treatment. The apparatus used in this work was NanoTest™ Platform by Micro Materials Ltd. This instrument monitors and records the load and displacement of a diamond three-sided pyramidal indenter tip with a radius of curvature of about 100 nm. A constant load of 10 μN has been applied. Scans (200 μm) were collected with the tip in close proximity to the surface, but not in contact. Nanoindenter is able to achieve sub-nanometric depth resolution in the horizontal plane. This resolution allows for the detection of changes to topography and providing valuable information on contribution of surface roughness to adhesion strength.

Two specimens of each film were randomly selected for recordings 20 measurements per sample. Average surface root means squared roughness (R_{RMS}) was calculated from equation 5 (Faibish et al., 2002).

$$R_{RMS} = \sqrt{\frac{\int_0^L (x_n - \bar{x})^2 dy}{L}} \tag{5}$$

Where x_n is the height of a random location on the scanned profile, x is the mean height of all measured heights and L is the sampling scan length.

3.7 Nano-indentation

Nano-indentation and nano-scratch techniques have been used in order to investigate the adhesion between organic substrate and inorganic layer.

Hardness and elastic modulus are calculated from the load vs. displacement data obtained by nano-indentation on coating at twenty different indentation depths ranging from 20m to 300 nm. NanoTest™ Platform, already described in section 3.6, monitors and records the dynamic load of a three-sided pyramidal diamond indenter. Berkovich tip with a radius of about 100 nm has been used.

In a indentation test, a Berkovich diamond tip is driven to indent the surface of the coating from the SiO_2 side. Tests were carried out in depth controlled mode, selecting a minimum and a maximum depth of 20 nm and 300 nm respectively. The experiments were performed with an initial load of 10 μN at loading and unloading rate of 10 μN/sec. The hold time of 30 sec at peak load was kept constant. Additional hold at 90% unload in all tests was set for thermal drift correction.

The indenter needs to be held at the constant indentation load for a certain amount of time in order to eliminate the dynamic effect and reach the quasi-steady flow state.

Each successive indent was displaced by 50 μm in order to avoid overlapping of plastic deformation zone onto neighbouring indents.

All data were corrected for thermal drift and instrument compliance and subsequently analysed with the Oliver and Pharr method (1992).

During the course of the instrumented indentation process, a record of the depth of penetration is made, and then the area of the indent is determined using the known geometry of the indentation tip. Indenting parameters, such as load and depth of penetration, can be measured. A record of these values can be plotted on a graph to create a load-displacement curve.

Figure 2 shows a typical loading and unloading displacement curves during a nanoindentation cycle on AryLite™. A power law curve was fit to the unload data points.

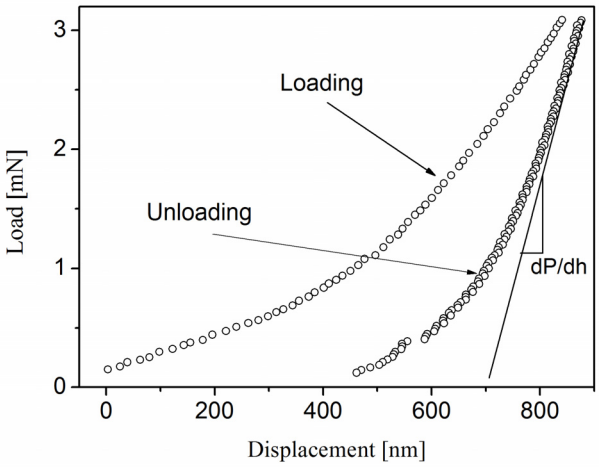

Fig. 2. Typical loading and unloading displacement curves during a nanoindentation cycle on AryLite™ substrate

The slope dP/dh at the maximum load data point is used to calculate the elastic modulus (Er). Hardness is calculated by dividing the loading force by the projected residual area of the indentation. Hardness and the Young's modulus of elasticity can be obtained from the slope of the unloading curve. The hysteresis indicates that the deformation is not fully elastic and partially inelastic.

3.8 Nano-Scratch test

In nano-scratch studies a conical indenter is drawn over the sample surface with ramping up of the load until damage occurs. The load corresponding to this damage provides a measure of scratch resistance or adhesive strength of a coating and is called the "critical load" (Park & Kwon, 1997). The definition of damage can be the onset of cracking around the scratching tip, spalling of the coating, or the formation of a channel in which all of the coating has been removed from the substrate. The critical loads are indicators of the scratch resistance of these samples.

Scratches have been made by translating the sample while ramping the loads on the conical diamond tip (1μm tip radius) over different load ranges from 0 mN to 10 mN. A sudden increase in the scratch load was related to coating damage.

Multipass test experiments have been performed. They consist of three sequential scans over the same 250 μm track, all at 2 μm/sec scan speed. In the first topography scan the applied load was constant at 100 μN. Surface roughness was measured from this scan. In the second scratch scan, the load applied after 50 μm was ramped at a constant rate of 0.1 mN/sec to a maximum load reached of 10 mN. In the final scan the resultant topography was observed by using a low applied load of 100 μN. Five repeat tests were performed on each sample.

4. Results and discussion

4.1 Thermo-Mechanical properties of AryLite™

AryLite™ exhibits excellent Tg (324°C) (figure 3) and good optical transparency. The lack of crystalline phase is a consequence of the aromatic and rigid nature of the polymer backbone which hinders conformational rearrangements into a regular crystalline structure. On the other hand the rigid backbone is responsible of reduced elongation at break and the lack of crystalline reinforcement results in poor elastic and ultimate properties (table 2).

The initial degradation temperatures (T_{id}) have been measured by using thermogravimetric analyser at a scanning rate of 10°C/min in N_2 purging flow. T_{id} is associated to 3 % weight loss.

Thermal and mechanical behavior of polyester indicate that AryLite™ is a good candidate for optoelectronic application.

Thermal and mechanical properties of AryLite™ are shown in table 2.

	AryLite™
Glass transition temperature T_g [°C]	324
Initial degradation temperature [°C]	488
Young's Modulus E_s [GPa]	2.82±0.24
Elongation at break ε_r [%]	10.24±2.56

Table 2. Thermo-mechanical properties of Arylite™

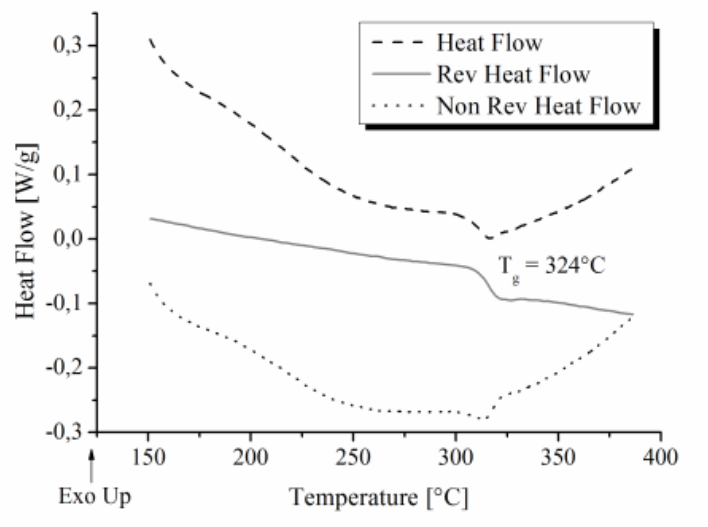

Fig. 3. Modulated Differential Scanning Calorimetry of AryLite™.

4.2 Spectroscopic analysis FTIR-ATR

Infrared spectroscopic analysis has been performed to verify the reaction between amino group located on the organo-silane and carboxylic group of polymeric substrate.

In figure 4 normalized ATR spectra of untreated AryLite™ and AryLite™ treated with APTEOS solution have been plotted.

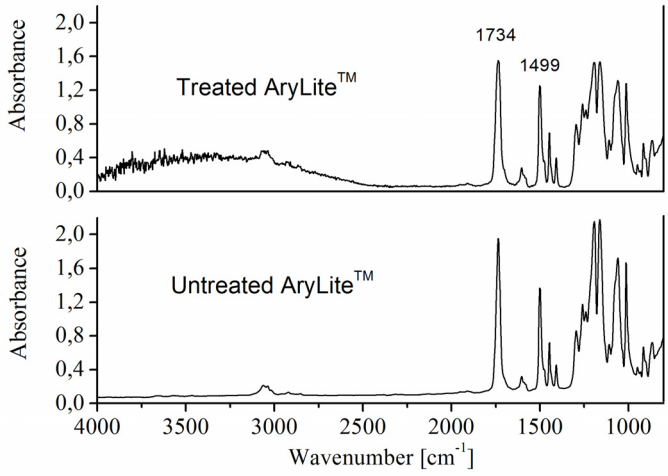

Fig. 4. ATR spectra of AryLite™ before and after surface silane treatment in the range 4000-700 cm^{-1}

In order to make a comparison between the treated and untreated samples the intensity of each peak was rationed (Gu et al., 2001) against the absorbance of the invariant band at 1499 cm^{-1}. These peaks are due to C-H in-plane bending of the benzene ring.
In the FTIR-ATR spectra, silane-treated specimens show a wide peak between about 2500 – 4000 cm^{-1}. This is attributable to the presence of SiOH groups (Anderson & Smith, 1974).
Treated sample spectra show a decrease of C=O ester linkage at 1734 cm^{-1} and a decrease of C–O ester stretching vibrations in the region 1300 – 1000 cm^{-1} after silane treatment (Bellamy, 1975) (Colthup et al., 1990).
This is attributable to nucleophilic addition of the amine group (NH_2) to the carbonilic group. Following this reaction path, the organosilane APTEOS has been grafted on the AryLite™ substrate.
In fact, a chemical reaction could happen between amine group (NH_2) of silane and carbonilic group of polymer substrate. The reaction produce an amide group (O=C-NH). This hypothesis has been supported by a spectroscopic study. Figure 5 shows double peak of amide group located at about 1640-1540 cm^{-1}.

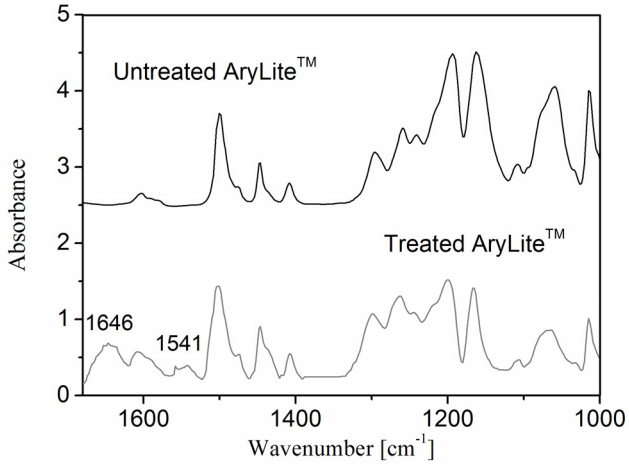

Fig. 5. FTIR spectra of polyarilate before and after silane treatment in a dichloromethane solution

4.3 Contact angle measurements

AryLite™ is an hydrophobic film with a water contact angle of 92 degrees. Samples treated with silane show a decrease of water contact angle of about 20 degrees. It has been demonstrated that silane treatment is effective in increasing the hydrophilicity of samples.

4.4 Evaluation of surface free energy (SFE)

In order to obtain γ_S^d and γ_S^p of a solid, contact angle data for a minimum of two known liquids are required. If two liquids are used, then, one must be polar and other is non-polar.
In this study two test liquids were used as a probe for surface free energy calculations: distilled water and ethylene glycol. The data for surface tension components of the test liquids at 20 °C are given in table 1.

Silane treatment binds OH groups on the polymeric surface. This phenomenon increase polyester surface polarity and surface free energy (Clint, 2001) (table 3). The increase in surface polarity causes an increase in molecular forces between substrates and hence an increase in adhesion strength (Burnett et al., 2007) (Comyn, 1992) (Lee & Wool, 2002).
In table 3 are reported SFE of untreated AryLite™ and treated AryLite™ calculated by using geometric mean method (Spelt et al., 1996).

	Surface Free Energy [mJ/m²]			
	γ	γ_S^d	γ_S^p	P
Untreated AryLite™	29.97	27.80	2.17	0.07
Treated AryLite™	30.19	17.10	13.09	0.43

Table 3. Surface free energy and polarity of AryLite™ films before and after surface treatment

4.5 Topography measurements

The topography scan technique was used to measure the roughness of samples before and after the silane treatments.
The changes of surface roughness produce a surface topography variation and provide a contribution to substrates adhesion strength.
Untreated AryLite™ films are smooth and they possess the lower roughness value of about 2.64±0.57 nm. Treated and untreated samples exhibit a root means squared roughness (R_{RMS}) lower than 20 nm. All materials can be considered as totally flat from a topographic point of view (Ponsonnet et al., 2003).
Clearly, surface roughness of the treated polymers was higher than the untreated polyester. After the chemical treatment AryLite™, exhibit a R_{RMS} value 2.7 times higher than unmodified material.
As expected, the silane treatment increase the surface roughness of polyester film.

4.6 Nano-indentation test

Nano-mechanical tests on SiO_2 layers deposited on AryLite™ have been carried out to further investigate the interface between organic substrate and inorganic layers.
Since coating of SiO_2 is less than 1 μm thick, small volume testing methods such as depth-sensing nano-indentation and nano-scratch were used as a indicator of film adhesion strength. Nano-indentation tests has been conducted with Berkovich tip, on 100 nm thick SiO_2 side deposited on AryLite™ substrates. Results are shown in figure 6.
The presence of rigid hard coating on soft substrate results in an depth sensitive properties. The variation of young's modulus (E) and hardness (H) with depth were plotted in figure 6(a) and 6(b).
As reported in figure 6(a) Young's modulus aren't greatly affected by compatibilizing treatment and the elastic modulus decrease with increase depth. Both polymer substrates exhibit the same elastic properties approximately 3.5 GPa for depth higher than 300 nm. Beyond this limit the elastic modulus is not influenced from the presence of the SiO_2 coating. This value is slightly higher than 2.9 GPa calculated by tensile test and reported in literature (Abdallah et al., 2008). According to Zheng et al. (2005) elastic modulus measured by depth sensing indentation are invariantly higher than tensile test by a value of 5-20%. The

difference between uniaxial and indentation results is probably attributable to the data reduction procedure used in analyzing the indentation data. If the polymer was creeping while unloading, this would tend to increase the slope of the unloading curve and hence the calculated elastic modulus.

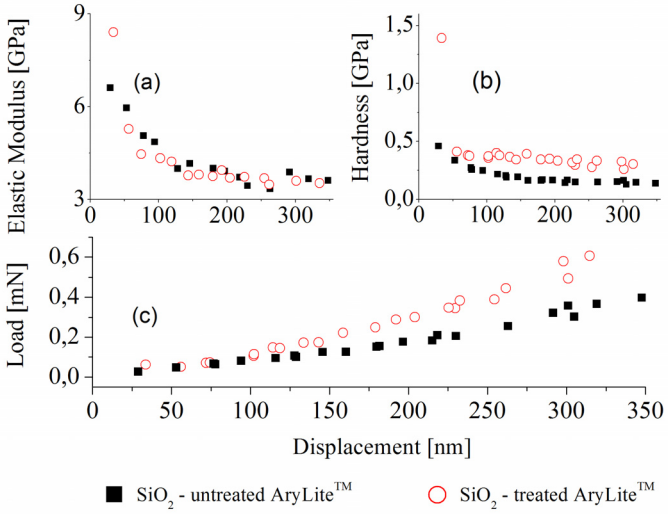

Fig. 6. Young's modulus (a), hardness (b) and load vs. depth (c) of untreated and treated AryLite™ coated with SiO_2 layer

The load applied to obtain depth higher than 100 nm was much greater for treated samples than for untreated substrate (Malzbender et al., 2002) (figure 6(c).

4.7 Nano-scratch test and Work of Adhesion

The polymer surface of AryLite™ has been modified to improve the adhesion between organic-inorganic layer and to reduce the inorganic layer cracking surface (Park & Jin, 2001) (Lian et al., 1995).

Depth of scratches with increasing normal load were measured in situ by topography scan of the film before and after the scratch event. Length of the test has been 250 µm. The load for initial and post scratch scan was 100 µN. In order to make effective use of the displacement data for production of a profile, it was assumed that region associated with the pre-scratch scan was unaffected by the deformation. Data from these regions were used to account for both the slope and curvature of the sample surface so that the entire scratch could be viewed with the surface of the sample as the baseline for deformation.

Five scratches were made at each load at different areas of specimen.

The load corresponding to the damage provides a measure of scratch resistance or adhesive strength of a coating and is called "critical load" (Lc) (Beake & Lau, 2005) (Beake et al., 2006) (Rats et al., 1999) (Zheng & Ashcroft, 2005) (Charitidis et al., 2000). Untreated AryLite™ exhibit a Lc value of 3.4±0.2 mN (figure 7); a 1 µm conical indenter has been used resulting in evident and reproducible data. The failure begins abruptly by brittle fragmentation and spallation in the coating. Spalling coating failure modes (Burnett & Rickerby, 1987) occurs as

a result of the compressive stress field preceding the moving tip. Spallation is the result of total delamination and adhesive failure.

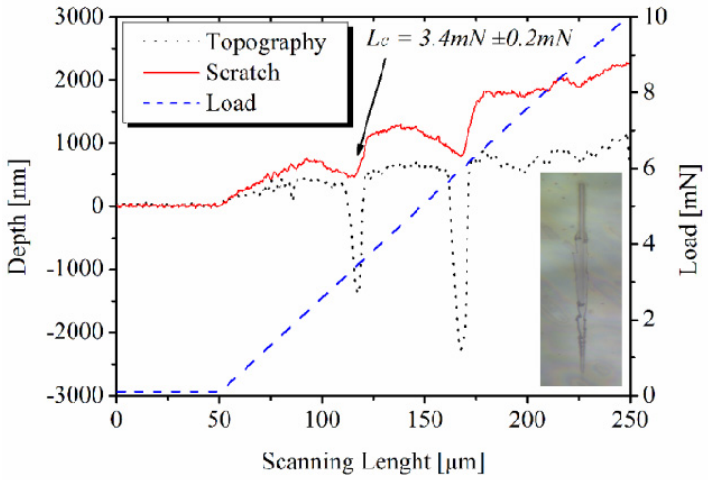

Fig. 7. Scratch test curve of SiO_2 layer of untreated AryLite™ with optical image in the plot inset (magnification 20x)

The scratch curve test of SiO_2 coating reveal that no inflexion can be found in depth curves of silane-treated samples which means that the films cannot be delaminated in the scratch process. Indeed, critical load disappeared after surface modification treatment, there is no abrupt change in the displacement curves, implying that the coatings did not peel off during the scratch ramping load (figure 8).

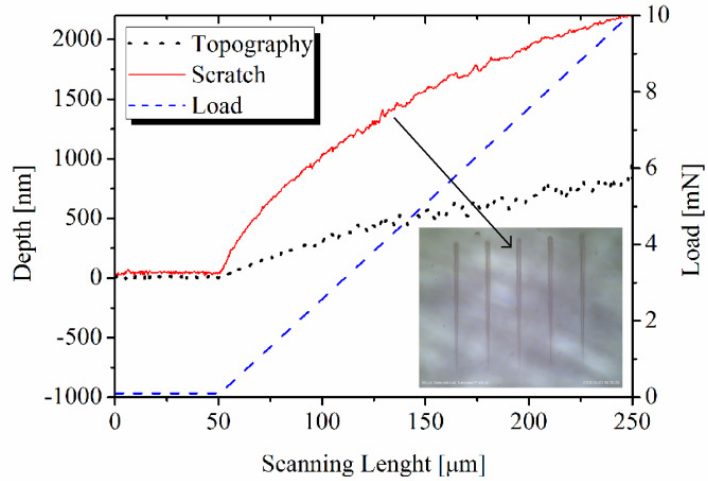

Fig. 8. Scratch test curve of SiO_2 layer of treated AryLite™ with optical image in the plot inset (magnification 20x). Topography and scratch scan refers to the third wear

A careful observation by optical microscopy has been made by comparing the topography pre-scan and post-scan to the scratch-scan for silane-treated and coated sample. The optical images reveal that the scratch is extremely smooth and shallow.
Similar observations performed at higher load confirm the same failure mechanisms. The scratch surface remains smooth until the wear exposes the polymer substrate. This is a conformal crack coating failure mode (Burnett & Rickerby, 1987)that consist of cracking within the scratch only and it occur when the coating remains fully adherent.
Evaluation of the adhesion strength between the coating and the substrate is complicated since it depends on a combination of many factors. In the first approximation, the adhesion can be modeled in terms of the strain energy released during fracture of the coating.
Griffith (1920) cast the problem of fracture in terms of energy balance. Griffith's study was based on the idea that all materials contain imperfections on a very small scale. Griffith's idea was to model a static crack as a reversible thermo-dynamical system. Equilibrium (i.e. no crack extension or contraction) is attained when over an infinitesimally small increase in crack length, dC, there is no overall change in energy of the system (U).
This can be expressed by Griffith energy balance concept:

$$\frac{dU}{dC} = 0 \tag{6}$$

Using a Griffith energy balance approach, the strain energy released provides the surface energy for a crack to form at the coating-substrate interface. The stress responsible for interface failure is related to the work of adhesion, W. Burnett and Rickerby (1987) have identified three contributions to the stress responsible for coating detachment: elastic-plastic indentation stress, internal stress and tangential frictional stress. In this model, the elastic-plastic indentation stress is considered to be dominant; the shear (frictional) stress is small compared with the ploughing (indentation) stress, they established the following relation:

$$W = \frac{32}{\pi^2} \frac{t \cdot L_c^2}{E_c \cdot w_c^4} \tag{7}$$

where w_c represents the width of the scratch track at the critical load, t and E_c is respectively the thickness and elastic modulus of inorganic coating.
In the case of a coating on polymer substrate, W increases with the film thickness. For unmodified and coated sample it has been found that W is about 0.18 J/m^2.
The proposed approach is not useful for the evaluation of W in the case of very strong interface.
The absence of critical failure for modified and coated sample has not allowed the experimental evaluation of Lc value, thus preventing the use of equation 7.
This is clearly evidenced by figure 7, where a scratch depth of 2000 nm have been reached without spallation.

5. Conclusion

In this paper polymer surface has been modified by chemical treatment in order to improve the adhesion properties. Coupling agent with amino functional group (3-Aminopropyl)triethoxysilane (APTEOS) has been grafted on polyester surface. A significant decrease of water contact angle have been measured for treated sample resulting in increased wettability and surface free energy of polymeric substrate. The increase of surface polarity enhance the adhesion of silicon dioxide subsequently deposited with Electron Cyclotron Resonance (ECR).
The improvement of adhesion is associated with the presence of SiO_x grafted on the surface. Small volume testing method, such as nano-indenter and nano-scratch, have been used to characterize interfaces of multilayer composite.
Nano-scratch test of SiO_2 layer of untreated AryLite™ exhibit a critical load (Lc) coupled with surface fractures, delamination and blistering. This is a clear evidence of a poor adhesion at the interface between substrate and inorganic films.
Critical load for SiO_2 detachment from treated sample was not observed, as a consequence of a different failure mechanism, due to surface modification. In fact, there is no abrupt change in the displacement curves, implying that the coatings did not peel off during the scratch ramping load scratch. The optical images reveal that the scratch is extremely smooth and shallow, implying that the coatings strongly adheres on substrate. The results showed that adhesion of SiO_2 on AryLite™ has been improved by substrate silane surface treatment.

6. Acknowledgements

The activities was performed in the framework of the project FIRB "Poliflex" (RBIP06SH3W) granted to IMAST S.c.a.r.l. The authors gratefully acknowledge Ferrania Imaging Technologies S.p.A. for providing AryLite™ substrates. The authors also wish to thank Mrs Marcedula M. and Mr De Angioletti M. for experimental tests.

7. References

Abdallah A.A., Bouten P.C.P., den Toonder J.M.J., de With G. (2008). The effect of moisture on buckle delamination of thin inorganic layers on a polymer substrate. *Thin Solid Films*, 516, 1063–1073.

Adhikari B., Majumdar S. (2004). Polymers in sensor applications. *Prog. Polym. Sci,* 29, 699–766.

Amendola E., Cammarano A., Pezzuto M., Acierno D. (2009). Adhesion of functional layer on polymeric substrates for optoelectronic applications. *Journal of the European Optical Society - Rapid publications*, 09027, 4, 1-6.

Anderson D.R., Lee Smith A. (1974). *Analysis of Silicones*. Wiley-Interscience editor, Chapter 10, New York.

Angiolini S., Avidano M. (2001). P-27: Polyarylite Films for Optical Applications with Improved UV-Resistance. *Organic Synthesis Lab. Polymers, Ferrania Imaging Technologies, Technical Information.*

Beake B.D., Lau S.P. (2005). Nanotribological and nanomechanical properties of 5-80 nm tetrahedral amorphous carbon films on silicon. *Diamond & Related Materials*, 14, 1535-1542.

Beake B.D., Ogwu A.A., Wagner T. (2006). Influence of experimental factors and film thickness on the measured critical load in the nanoscratch test. *Materials Science and Engineering A* 42, 70-73.

Bellamy L.J. (1975). The infrared spectra of complex molecules. John Wiley & Sons, 3rd ed., p.49, New York.

Burnett P.J. and Rickerby D.S. (1987). The relationship between hardness and scratch adhesion. *Thin Solid Films*, 154, 403-416.

Burnett D., Thielmann F., Ryntz R. (2007). Correlating thermodynamic and mechanical adhesion phenomena for thermoplastic polyolefins. *Journal of Coatings Technology and Research*, 4, 2, 211-215l.

Cantin S., Bouteau M., Benhabib F. and Perrot F. (2006). Surface free energy evaluation of well-ordered Langmuir–Blodgett surfaces Comparison of different approaches. *Colloids and Surfaces A: Physicochem Eng. Aspects,* 276, 107-112.

Charitidis C., Logothetidis S., Gioti M. (2000). A comparative study of the nanoscratching behavior of amorphous carbon films grown under various deposition conditions. *Surface and Coatings Technology*, 125, 201–206.

Choi M.C., Kim Y., Ha C. S. (2008). Polymers for flexible displays: From material selection to device applications. *Prog. Polym. Sci,* 33, 581–630.

Clint J. H. (2001). Adhesion and components of solid surface energies. *Current Opinion in Colloid & Interface Science*. 6, 28-33.

Colthup N.B., Daly L.H., Wiberley S.E., Introp P. (1990). Introduction to infrared and Raman spectroscopy. Academic, 3rd ed., p 94.

Comyn J. (1992). Contact Angles and Adhesive Bonding. *International Journal of Adhesion and Adhesives*, 12, 3, 145–9.

Faibish R.S., Yoshida W., Cohen Y. (2002). Contact Angle Study on Polymer-Grafted Silicon Wafers. *Journal of Colloid and Interface Science,* 256, 341 – 350.

Fowkes F.M. (1962). Determination of interfacial tensions, contact angles, and dispersion forces in surfaces by assuming additivity of intermolecular interactions in surfaces. *Journal of Physical Chemistry*. 66, 2, 382.

Goddard J.M., Hotchkiss J.H. (2007). Polymer surface modification for the attachment of bioactive compounds. *Progress in Polymer Science*, 32, 698-725.

Griffith (1920). The phenomenon of rupture and flow in solids. *Philosophical Transactions of the Royal Society of London*, 221, 163.

Gu X., Raghavan D., Nguyen T., VanLandingham M.R., Yebassa D. (2001). Characterization of polyester degradation using tapping mode atomic force microscopy: exposure to alkaline solution at room temperature. *Polymer Degradation and Stability*, 74, 139–149.

Imparato A., Minarini C., Rubino A., Tassini P., Villani F., Guerra A., Amendola E., Della Sala D. (2005). Thin silicon films on polymeric substrates. *Macromol. Symp,* 228, 167-176.

Lee I., Wool R.P. (2002). Thermodynamic Analysis of Polymer-Solid Adhesion: Sticker and Receptor Group Effects. *Journal of Polymer Science Part B: Polymer Physics*, 40, 20, 2343–53.

Lian Y.M., Leu K.W., Liao S.L., Tsai W.H. (1995). Effects of surface treatments and deposition conditions on the adhesion of silicon dioxide thin film on polymethylmethacrylate. *Surface and Coatings Technology*, 71, 142-150.

Ma Z., Mao Z., Gao C. (2007). Surface modification and property analysis of biomedical polymers used for tissue engineering. *Colloids and Surfaces B: Biointerfaces*, 60, 137–157.

Mack G.L. (1936). Determination of contact angles from measurements of the dimension of small bubbles and drops. I. The spheroidal segment methods for acute angles. *J Phys Chem*, 40, 159-167.

Malzbender J., den Toonder J.M.J., Balkenende A.R., de With G. (2002). Measuring mechanical properties of coatings: a methodology applied to nano-particle-filled sol-gel coatings on glass. *Materials Science and Engineering*, 36, 47-103.

Mannifacier J.C., Szepessy L., Bresse J.F., Perotin M., Stuck R. (1979). In_20_3:(Sn) and SnO_2:(F) films–Application to solar energy conversion; part 1 – preparation and characterization. *Mater. Res. Bull,* 14, 163.

Oliver W.C., Pharr G.M. (1992). An improved technique for determining hardness and elastic-modulus using load and displacement sensing indentation experiments. *Journal of Materials Research*. 7, 1564-83.

Owens D.K., Wendt R.C. (1969). Estimation of the surface free energy of polymers. *J. Appl. Polym. Sci.*, 13, 1741–1747.

Ozcan C., Hasirci N. (2008). Evaluation of Surface Free Energy for PMMA Films. *Journal of Applied Polymer Science*, 108, 438–446.

Park H.S., Kwon D. (1997). An energy approach to quantification of adhesion strength from critical loads in scratch tests. *Thin Solid Films*. 307, 156-162.

Park S.J. and Jin J.S. (2001). Effect of Silane Coupling Agent on Interphase and Performance of Glass Fibers/Unsaturated Polyester Composites. *Journal of Colloid and Interface Science*, 242, 174–179.

Ponsonnet L., Reybier K., Jaffrezic N., Comte V., Lagneau C., Lissac M., Martelet C., (2003). Relationship between surface properties (roughness, wettability) of titanium and titanium alloys and cell behaviour*Materials Science and Engineering C*, 23, 551.

Rats D., Hajek V., Martinu L. (1999). Micro-scratch analysis and mechanical properties of plasma-deposited silicon-based coatings on polymer substrates. *Thin Solid Films*, 340, 33-39.

van Oss C.J., Good R.J., Chaudhurys M.K. (1988). Additive and Nonadditive Surface Tension Components and the Interpretation of Contact Angles. *Langmuir*, 4, 884-891.

Young T. (1805). An Essay on the Cohesion of Fluids. *Philosophical transactions Royal Society London*. 95, 65-87.

Zhao Q., Liu Y., Abel E.W. (2004). Effect of temperature on the surface free energy of amorphous carbon films. *Journal of Colloid and Interface Science*, 280, 174–183.

Zheng S., Ashcroft I.A. (2005). A depth sensing indentation study of the hardness and modulus of adhesives. *International Journal of Adhesion & Adhesives*, 25, 67–76.